

# Estimating Rooftops' Suitability for PVs Using Pleiades-1B Satellite Image for Charging Electric Vehicles in New Cairo, Egypt.

Shaimaa Ahmed, Mohamed Amr Serag-Eldin, and Mohamed El-Morsi

American University in Cairo, New Cairo (Egypt)

## Abstract

Studying the potential of solar energy PV rooftops requires assessing solar energy and rooftop areas. First, solar radiation data on a horizontal surface were obtained from a weather station in New Cairo City (Egypt). Second, the Hay & Davies, Klucher, and Reindl (HDKR) model was used to calculate the available solar radiation on tilted surfaces. Finally, rooftops were identified and extracted from a Very High-Resolution (VHR) satellite image using Remote Sensing and Geographic Information Sciences techniques. The flat rooftops' extraction accuracy ranged between 74.6% and 96.875%. The area required for generating enough energy for one Electric Vehicle (EV) was estimated for both summer and winter. Avoiding shades from parapet walls and following the country's building codes, the water tanks and rooftop rooms were considered for PV installation. The results showed that PV rooftops could provide electricity for charging EVs in neighborhoods with different urban designs. The variables affecting the solar energy potential for EV charging are suitable rooftop areas and available solar radiation.

*Keywords: PVs, rooftops, urban, neighborhoods, HDKR model, Remote Sensing, Geographic Information Sciences, very high-resolution satellite images, electric vehicles*

---

## 1. Introduction

Rooftops are essential for producing solar energy using PVs in urban areas. Desert cities such as the new administrative capital (*New Administrative Capital's Map In Detail And Its Scheme*, 2019), Six of October City (*October 6*, 2022), and New Cairo City (*New Cairo*, 2022) in Egypt can benefit a lot from the abundance of solar energy (*Solar Resource Maps of Egypt*, 2019), (*Global Solar Atlas*, 2019), especially since their topography is almost horizontal. The height of buildings is almost equal in many neighborhoods and districts due to the planning laws for new cities in Egypt. However, generating solar energy from PVs installed on the rooftops of buildings is not well implemented in Egypt, and there is a lack of information about the rooftops. Therefore, mapping rooftops using VHR satellite images is important because the information is up to date, and it has more accurate measurements of the roofs.

Geographic Information Sciences (GIS) and Remote Sensing (RS) are used to detect and calculate suitable rooftop areas for generating electricity using PVs. Gassar & Cha (2021) reviewed and demonstrated 265 studies from all over the world and included one study only about solar PVs generated from rooftops in Egypt (Aboushal, 2018). In his paper, Aboushal (2018) introduced a method to identify possible rooftop areas for PVs and how to select the optimum PVs. The suggested method combined the probabilistic approach and spatial analysis to compute PV's Power Capacity Factor (PCF). The highest PCF score was selected for use in the defined urban Area in Alexandria Governorate, Egypt. Their method was based on three steps: digitizing the urban Area from Google Earth using ArcGIS, comparing PVs based on their PCF, and linking maps and PCF data.

Based on the literature survey, very few detailed research studies map suitable rooftop areas for PV installation in urban areas in Egypt. For example, Taha et al. (2021) automatically identified tourist chalets from one Pleiades satellite image for Marina Resort in Egypt. They classified the satellite image using several machine learning algorithms, namely Random Forest (RF), Maximum Likelihood (ML), Support Vector Machines (SVM), and Backpropagation Neural Networks (BNN). After running these algorithms for obtaining urban and non-urban classes, they applied different morphological operations and Sobel Edge Detection techniques and conducted the quality analysis. It was concluded that RF has the highest overall accuracy and scored 97%. ML scored 95%, SVM scored 93%, and BNN scored 92%. Muhammed et al. (2021) used gamma correction, vegetation and shadow masking, k-means, and connected features, and SVM classification was applied to a satellite image to detect rooftops on an image from Google Earth Pro. They removed the shades by creating a shades index and trained the model using digitized buildings. The accuracy assessment of SVM was 95%, and the annual PV potential was projected to be between 9.3 and 8.7 MWh/year.

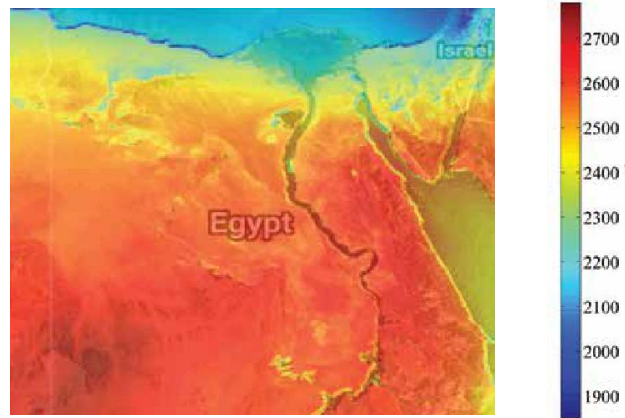
Many studies investigated how solar energy could be invested in creative ways such as charging Electric Vehicles (EVs) or storing generated energy in batteries of EVs (Aljohani et al., 2020; Chandra Mouli et al., 2020; Ghotge et al., 2020; Kawamura & Muta, 2012; Mohammad et al., 2020; Vermeer et al., 2020). However, little research was conducted in the Middle East, North Africa (Alsomali et al., 2017), or Egypt (Hassan & Abdellatif, 2021; *Improving Electric Vehicle Performance Using Photovoltaic Cells*, 2018). Moreover, Egypt is developing new creative solutions to cope with the increased energy demand (Egypt, 2021; *Energy Consumption in Egypt*, 2020; *Energy Consumption in Egypt*, 2020; *Renewable Energy Outlook*, 2018; El-Kholy & Faried, 2011). Egypt developed a new policy towards EVs which will increase EVs usage, importing EVs (EGYPT'S EVOLVING POLICY FRAMEWORK FOR ELECTRIC VEHICLES, 2020; Energy Efficiency and Renewable Energy Strategies and Policies, 2019; POLICY BRIEF: Mainstreaming Electric Mobility in Egypt: Seeing the Bigger Picture of Sustainable Cities, 2020), and manufacturing Egyptian EVs (FEV Group GmbH, 2022; State Information Service, 2022).

The optimal orientation and inclination of PVs could be horizontal or tilted on the rooftops. It is recommended that the tilted angle equals the location's latitude to obtain the maximum solar irradiance (How Does the Tilt Angle and/or Orientation of the PV Panel Affect System Performance? | Photovoltaic Lighting | Lighting Answers | NLRIP, 2021; National Solar Radiation Data Base Daily Statistics Files. National Renewable Energy Laboratory, 2005). Also, it is recommended that PVs face south in the northern hemisphere. The Hay, Davies, Klucher, and Reindl (HDKR) model (Duffie & Beckman, 2013) is highly recommended to be used when the only available data is the global solar radiation data on a horizontal surface.

It is strategic to investigate mapping rooftops to harvest energy generated from PVs to charge EVs in Egypt (Electric Vehicle Charging, 2021). This pilot study aims to map suitable areas using Pleiades-1b satellite images for PV rooftops to charge EVs. The study is conducted on compound scales in New Cairo city, and it uses solar irradiation data collected from a pyranometer located at the American University in latitude and longitude angles of 30° and 31.5°, respectively (Latitude, 2022).

According to Fakhraian et al. (2021), the hierarchical approach for estimating Solar potential on rooftops includes four stages. These stages include estimating physical potential (horizontal solar radiation), considering geographic potential (the built-up environment's impact), and estimating technical potential (the potential of generating electricity). In addition, the economic potential could be added, and it is the evaluation of the economic

attractiveness of PV rooftops under the present market situation. This paper demonstrates the findings for the physical and geographic potential only. Future research will discuss the technical PV potential and economic potential (Fig. 1).



Map. 1. Egypt mean surface energy potential Adopted from (Kosmopoulos & El-Askary, 2019)

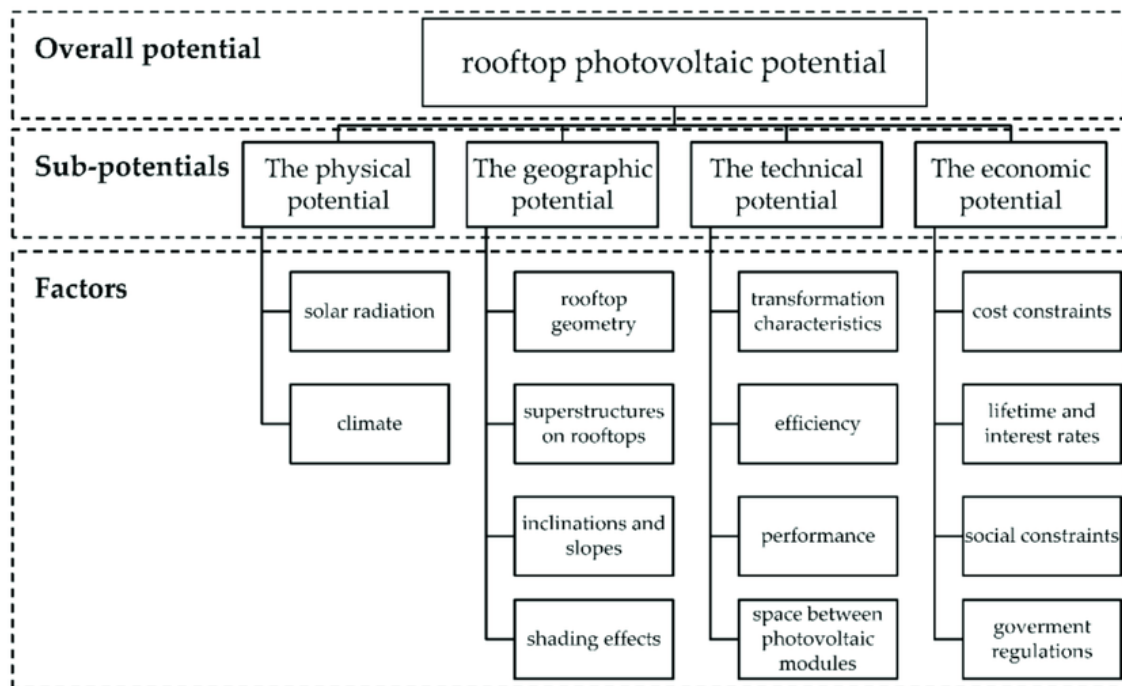


Fig. 1. Hierarchical methodology for estimating Solar potential on rooftops (Fakhraian et al., 2021)

## 2. Methods

### 1. Meteorological data

The total irradiance,  $G$ , on a horizontal surface, is measured and averaged every hour, in  $W/m^2$ , using a pyrometer, model CMP10, and manufactured by KIPP & ZONEN (CMP10 Secondary Standard Pyranometer, CMP10 - Kipp & Zonen, 2010). The data was collected for three years, from the end of 2018 to the beginning of 2021.

The HDKR model (Duffie & Beckman, 2013) is utilized to calculate the hourly irradiation on a tilted surface in  $kWh/m^2$ ,  $I_T$ , as shown by Eq. 1, (Duffie et al., 2020). The surface is south facing and tilted at a slope  $\beta = 30^\circ$  from the horizontal.

$$I_T = (I_b + I_d A_i) R_b + I_d (1 - A_i) \frac{(1 + \cos \beta)}{2} \left[ 1 + f \sin^3 \left( \frac{\beta}{2} \right) \right] + I \rho_g \frac{(1 - \cos \beta)}{2} \quad (\text{eq.1})$$

$I_d$  is the hourly diffuse irradiation in  $kWh/m^2$ , calculated using Eq. 2, Erbs' model (Estimation of the Diffuse Radiation Fraction for Hourly, Daily and Monthly-Average Global Radiation - ScienceDirect, 1982).

$$\frac{I_d}{I} = \begin{cases} 1 - 0.09k_T & \text{for } k_T \leq 0.22 \\ 0.9511 - 0.1604k_T + 4.388k_T^2 - 16.638k_T^3 + 12.336k_T^4 & \text{for } 0.22 < k_T \leq 0.80 \\ 0.165 & \text{for } k_T > 0.8 \end{cases} \quad (\text{eq.2})$$

where  $k_T$  is the hourly clearness index defined as the ratio of the hourly global (beam and diffuse) irradiation,  $I$ , received on a horizontal surface to the hourly radiation that would be received on a parallel extraterrestrial surface,  $I_o$ , as shown by Eq. 3 (Twidell & Weir, 1986)

$$k_T = \frac{I}{I_o} \quad (\text{eq.3})$$

The global irradiation,  $I$  is calculated by integrating the total irradiance,  $G$  over an hour. The hourly values of the total irradiance,  $G$  on a horizontal surface, are available from the pyranometer measurements. While,  $I_o$ , is the integration of the solar radiation incident on a horizontal plane outside of the atmosphere,  $G_o$ , over an hour calculated according to Eq. 4 (Duffie & Beckman, 2013).

$$G_o = G_{sc} \left( 1 + 0.033 \cos \frac{360n}{365} \right) \cos \theta_z \quad (\text{eq.4})$$

Where  $G_{sc} = 1.367 \text{ kW/m}^2$  is the solar constant,  $n$  is the day of the year, and  $\theta_z$  is the zenith angle.

In Eq. 1, the hourly beam irradiation  $I_b$  in  $kWh/m^2$ , is the difference between the hourly global irradiation,  $I$  received on a horizontal surface, and the hourly diffuse irradiation  $I_d$

In Eq. 1,  $f$  is a modulating factor defined as  $\sqrt{\frac{I_b}{I} \frac{(1 + \cos \beta)}{2}}$ , is the view factor for the tilted surface to the sky, and

$I \rho_g \frac{(1 - \cos \beta)}{2}$  is the view factor for the tilted surface to the ground (Duffie & Beckman, 2013).  $\rho_g = 0.2$  is the ground albedo.  $R_b$  is the ratio of beam radiation on the tilted surface  $G_{b,T}$  to that on a horizontal surface  $G_b$  at any time, as defined by Eq. 5 (Duffie & Beckman, 2013)

$$R_b = \frac{G_{b,T}}{G_b} = \frac{G_{b,n} \cos \theta}{G_{b,n} \cos \theta_z} = \frac{\cos \theta}{\cos \theta_z} \quad (\text{eq.5})$$

Where  $\theta$  is the angle of incidence, and  $\theta_z$  is the zenith angle.

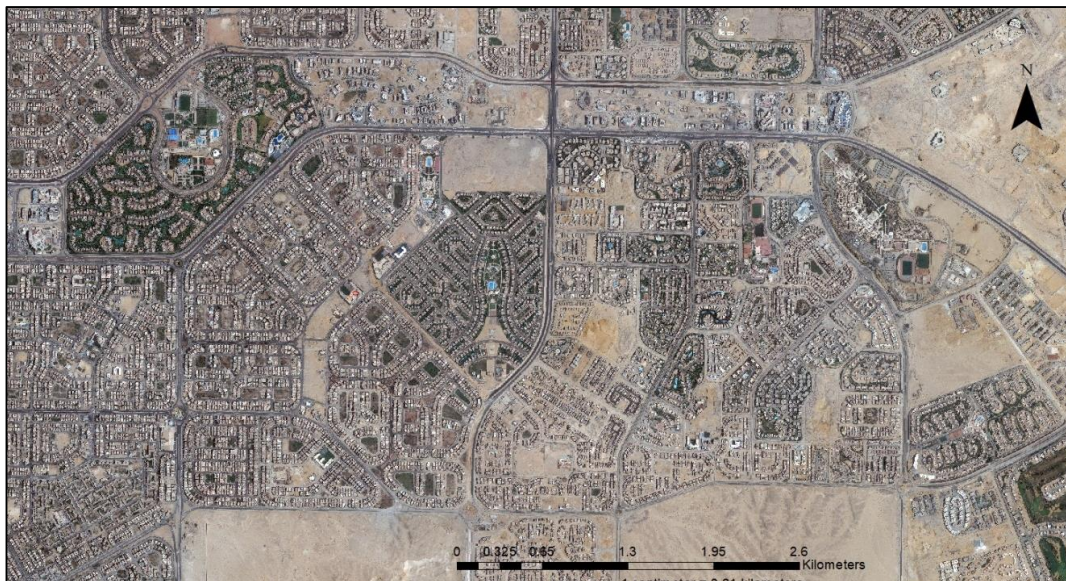
Finally,  $A_i$  is the anisotropy index,  $A_i$  is a function of beam radiation's atmospheric transmittance. It determines the portion of horizontal diffuse to be treated as forward scattered; it is incident at the same angle as beam radiation.

Under clear conditions,  $A_i$  is high, and most of the diffuse are forward scattered; when the sky is totally overcast,  $A_i = 0$ , and diffuse is isotropic.  $A_i$  is calculated as in Eq. 6 (Duffie & Beckman, 2013)

$$A_i = \frac{I_{b,n}}{I_{o,n}} = \frac{I_b}{I_o} \quad (\text{eq.6})$$

## 2. Pleiades-1B Satellite image data

The Pleiades-1B satellite image has a panchromatic band with a resolution of 50 cm (wavelength = 480-830 nm) and four multicolored bands. These bands are Blue (430-550 nm), Green (490-610 nm), Red (600-720 nm), and near-infrared (750-950 nm) bands, and their spatial resolution is 2 m (*Pleiades-1B Satellite Sensor / Satellite Imaging Corp, 2022*). The satellite image was taken on August 8, 2018. The pre-processing steps included enhancing the resolution of the satellite image and digitizing part of it. The panchromatic band increases the resolution of the multicolored bands in a process called pan-sharpen (*Earth Matters - How to Pan-Sharpen Landsat Imagery, 2017; Geometric Correction, Pan-Sharpening and DTM Extraction – Pleiades Satellite – CATALYST.Earth, 2022*). The resolution of the enhanced image is 0.5 m. After improving the spatial resolution, part of the image was digitized by ArcGIS software (*GIS Mapping Software, Location Intelligence & Spatial Analytics / Esri, 2019*). Next, the workflow involves extracting rooftops by applying a feature extraction module or supervised classification using RF and SVM algorithm on the cloud (*Catalyst Professional – CATALYST.Earth, 2021*), comparing the two overall accuracies, and selecting the highest accuracy results or digitized maps for mapping.



**Map. 2. Pleiades-1B satellite image for the study area after enhancement**



Map. 3. Rooftops design in one of the samples



Map. 4. Rooftops design in one of the samples



Map. 5. Rooftops design in one of the samples



Map. 6. Rooftops design in one of the samples

### 3. Estimating required areas for generating electricity from rooftops

Estimating the required area to generate energy for a car is based on the average daily irradiation, the average daily electric energy required by the car for July and December.

The average measured daily irradiation, on a horizontal surface, during July is  $H_{\text{July}} = 7.69 \frac{\text{kWh/m}^2}{\text{d}}$ . Consequently, the average daily electric energy produced by the selected PV is  $E_{\text{PV}}|_{\text{July}} = 1.3 \frac{\text{kWh/m}^2}{\text{d}}$ .

Assuming that the average electric energy required by an electric vehicle to travel 100 km is 15 kWh. For an average daily distance of 50 km, the average electric energy required by the car is  $E_{\text{car}} = 7.5 \text{ kWh/d}$ .

Thus, the PV area required per vehicle during July is  $A_{\text{PV}}|_{\text{July}} = \frac{E_{\text{car}}}{E_{\text{PV}}|_{\text{July}}} = \frac{7.5}{1.3} = 5.77 \text{ m}^2/\text{car}$ .

For December,  $H_{\text{Dec}} = 3.09 \frac{\text{kWh/m}^2}{\text{d}}$ . Consequently, the average daily electric energy produced by the selected PV is  $E_{\text{PV}}|_{\text{Dec}} = 0.56 \frac{\text{kWh/m}^2}{\text{d}}$ . Thus, the PV area required per vehicle during December is  $A_{\text{PV}}|_{\text{Dec}} = \frac{7.5}{0.56} = 13.39 \text{ m}^2/\text{car}$ . The PV areas required for July and December at different tilted angles are presented in Table 2

## 3. Results

### 1. Rooftops extraction

The feature extracting module, which is a part of professional catalyst software, managed to extract some of the rooftops accurately. After applying the classification function, the SVM tends to produce higher overall accuracy than the RF's algorithm, and the overall accuracy for the sample ranged between 74.6% and 96.87%. This accuracy range could be due to the overlap between the spectral signatures of different materials in urban areas. For example, the spectral reflectance of soil could be overlapped by the spectral signature of the rooftop's materials. In addition, the rooftops of buildings in desert cities could be covered by dust due to the sandy winds, and the sand's spectral signature is the same as the ground's top layer, sand. Moreover, the rooftops in one compound could be covered by different roof materials, requiring more rooftop types in the classification. Therefore, increasing the accuracy requires adding more classes and samples in the classification process.

To get accurate measurements for the suitable area of the rooftops', digitized maps were used. To avoid shades, the roofs of rooms or water tanks located on the rooftops were used and not the whole roof.



Map 7. The original Satellite image of one neighborhood



Map 8. Classified map using SVM



Legend

Table 1. 3Classification accuracy assessment for one compound

Accuracy Statistics						
Overall Accuracy		: 96.875%	95% Confidence Interval (		91.831%	100.000%)
Overall Kappa Statistic:		0.960				
Class Name	Producer's Accuracy	95% Confidence Interval	User's Accuracy	95% Confidence Interval	Kappa Statistic	
shades	100.000%	( 97.059% 100.000%)	94.444%	( 81.085% 100.000%)	0.9243	
street	84.615%	( 61.156% 100.000%)	100.000%	( 95.455% 100.000%)	1.0000	
Green	100.000%	( 93.750% 100.000%)	100.000%	( 93.750% 100.000%)	1.0000	
ground	100.000%	( 97.222% 100.000%)	94.737%	( 82.065% 100.000%)	0.9268	
roof2	100.000%	( 91.667% 100.000%)	100.000%	( 91.667% 100.000%)	1.0000	
Roof1	100.000%	( 75.000% 100.000%)	100.000%	( 75.000% 100.000%)	1.0000	
Quantity Disagreement:		3.125%	Allocation Disagreement:		0.000%	

Table 1 illustrates the accuracy assessment for a neighborhood, its producer user's accuracy, kappa statistics for each class, and the overall accuracy. The overall accuracy of the SVM classification is 97.876, and urban classes are rooftops, green areas, streets, bare soil, and shades. Producer's accuracy is the number of referenced locations classified correctly / the total number of reference locations for a specific class. User's accuracy is the total number of correct classifications for a specific class/row total of the accuracy matrix. Kappa statistics evaluate how well the classification performed in comparison to randomly assigned values for this class (*Accuracy Metrics*, 2019).

## 2. Required rooftops area for one car

The PV area required for July & December at different tilted angles  $\beta = 10^\circ, 20^\circ, 30^\circ, \text{ and } 45^\circ$  are presented in Table 2

**Table 2. Estimated required area for a car for the summer and winter at different tilted angles.**

Month	$\beta=0^\circ$	$\beta=10^\circ$	$\beta=20^\circ$	$\beta=30^\circ$	$\beta=45^\circ$
$A_{PV} _{July} \text{ m}^2/\text{car}$	5.8	5.9	6	6.5	7.5
$A_{PV} _{Dec} \text{ m}^2/\text{car}$	13.4	11.4	10.2	9.3	8.7

In the summer, the area required for charging one electric vehicle increases when the tilted angle of the PVs increases, and the area required for charging one electric vehicle decreases when the tilted angle increases in the winter. The area difference between summer and winter could limit the number of cars charged during the year to the number of cars charged in the winter only. Moreover, the additional energy generated in the summer could be exported to the grid.

### 3. Calculating how much cars could be charged in each compound

To get the maximum energy and avoid shades, tanks or rooms on the roofs are considered, and PVs arrangement facing south (Fig. 2).



**Fig. 2 Example of PVs Arrangement on Roof Tops  $\beta = 30^\circ$  (tech waves, 2019)**

**Table 3. Available area for charging EVs and how many cars could get enough energy based on the PV's tilted angle.**

Compound number	Approx. Area in $\text{m}^2$	Number of cars in Summer				
		At $\beta=0^\circ$	At $\beta=10^\circ$	At $\beta=20^\circ$	At $\beta=30^\circ$	At $\beta=45^\circ$
1	1301	226	222	214	202	174
2	536	93	91	88	83	72
3	3441	596	586	567	533	460
4	3574	620	609	589	554	478
5	288	50	49	47	45	38
6	3325	576	566	547	515	445

Table 3 illustrates the compound number of the sample data, the available rooftops area in each compound, and the number of Electric Vehicles that could be charged in the summer for different tilted angles, where  $\beta = 0^\circ, 10^\circ, 20^\circ, 30^\circ$  and  $45^\circ$ . The number of cars for each tilted angle = the total available area of rooftops of all buildings (before approximating the total available area) in a compound / the estimated required area for a car for the summer (Table 2)

**Table 4. Available area for charging EVs and how many cars could get enough energy based on the PV's tilted angle**

Compound number	Approx. Area in m <sup>2</sup>	Number of cars in winter				
		At $\beta = 0^\circ$	At $\beta = 10^\circ$	At $\beta = 20^\circ$	At $\beta = 30^\circ$	At $\beta = 45^\circ$
1	1301	97	114	128	139	150
2	536	40	47	53	57	62
3	3441	257	301	339	369	397
4	3574	267	313	352	383	412
5	288	21	25	28	31	33
6	3325	248	291	327	356	383

Table 4 illustrates the compound number of the sample data, available rooftops area, and the number of Electric Vehicles that could be charged in the winter for different tilted angles, where at  $\beta = 0^\circ, 10^\circ, 20^\circ, 30^\circ$  and  $45^\circ$ . The number of cars for a tilted angle = the total available area of rooftops of all buildings (before approximating the total available area) in a compound / the estimated required area for a car for the winter (Table 2)

In the summer, the number of cars that PVs could charge decreases with the increase of the inclined angle  $\beta$ . The number of EVs that could be charged is the maximum when PVs are horizontal. In the winter, the number of cars that PVs could charge increases with the inclined angle  $\beta$ , and the number of EVs that could be charged is maximum when PVs when  $\beta = 45^\circ$ . This suggests two scenarios for PV arrangements: arranging the PVs horizontally or at a tilted angle at  $\beta = 45^\circ$  after considering whether or not there is a plan to export the extra electricity to the grid.

#### 4. Discussion

Using one VHR satellite image in extracting rooftop areas automatically or semi-automatically is very promising in regions with urban features with discriminating spectral reflectance. However, extracting rooftops areas is challenging in desert regions where spectral reflectance of the materials of rooftops, pedestrians, streets, and bare land are overlapped (Mohamed, 2018), (Herold et al., 2004) and (Javed et al., 2021). Therefore, it is recommended to use three images to create a third dimension which can be used as a variable or an input in automatic or semi-automatic extraction (Tian et al., 2017), (Xiang et al., 2012), (Tian et al., 2017), and (ZuWhan Kim et al., 2001). Manual extraction or digitizing rooftops produces accurate measurements but is time-consuming and costly. The design of roofs in Egypt creates an additional challenge for mapping shades. For example, the thickness of the roof's parapet is 25 cm, and its height ranges between 90 cm and 1 m. Since the parapet's width (25 cm) is less than the spatial resolution (50 cm), it was not possible to detect the parapet (0.25 pixels) or its shades (less than 2 pixels). New Cairo's topography is almost horizontal and buildings heights are almost equal because of the construction Egyptian law. However, this is not the case all over greater Cairo where buildings' height and topography of the land are changing within the same block or neighborhood. Therefore, traditional civil surveying is important to identify the height of buildings (Shaker et al., 2011) to avoid shades created by other buildings.

It is essential to avoid shades that will decrease the efficiency of the PV. Shades' avoidance is possible by grouping PVs as one block array (Fig. 2) facing south. Therefore, developing more detailed designs or architecture drawings for PV arrangements facing south with acceptable height for each building with a unique rooftop design is required. Furthermore, not all designs and shapes of rooftops were taken into consideration. Since New Cairo's

architectural style is designed as a mixture of the Egyptian and Western styles, many shapes and designs exist for entirely or partially tilted rooftops. Suitable rooftops design should be enforced or recommended in new desert cities to achieve the best usage of rooftops for generating energy, a.

There is a high need for accurate information about EVs, the location of charging stations, and the number of families, buildings, and cars in each compound, and the average distance a driver takes daily to get accurate areas required for charging one EV. These requirements suggest creating extensive databases and spatial databases for EVs. Since EVs market has just started, it is suggested to create this database for each new EV that enters Egypt and update it throughout the year.

## 5. Conclusion

Rooftops can provide enough energy for charging EVs based on two factors, the available areas of rooftops not affected by the shades and the PVs` tilted angle. VHR satellite imagery provides a wealth of information for solar planning in urban areas for desert cities in Egypt. It could be used to map urban areas such as rooftops, streets, pedestrians, and parking. VHR satellite imagery could be used for estimating suitable areas for PV installation. Accordingly, estimating energy from PVs and the area required for charging one EV is possible. Remote Sensing and GIS are recommended for use in the different stages of planning and managing cities.

The current study identified and extracted rooftops in New Cairo-Egypt from VHR satellite images using Remote Sensing and Geographic Information Sciences techniques. The area required for generating enough energy for charging one EV was estimated for both summer and winter. The results showed that rooftops could provide electricity for charging EVs in neighborhoods with different urban designs. The maximum number of EVs depends on the available area in each compound, the time of the year, and the PV tilt angle.

## 6. Acknowledgments

This research was supported by the American University in Cairo (SSE-ENVE-S.A-FY22-CTSG-2022-Apr-10-11-48-48 and SSE-ENVE-S.A-FY17-RSG-2019-Feb-10-01-20-3)

## 7. References

- 6th October. (2022). [http://www.newcities.gov.eg/english/New\\_Communities/October/default.aspx](http://www.newcities.gov.eg/english/New_Communities/October/default.aspx)
- Aboushal, E. A. (2018). Applying GIS Technology for optimum selection of Photovoltaic Panels “Spatially at Defined Urban Area in Alexandria, Egypt.” *Alexandria Engineering Journal*, 57(4), 4167–4176. <https://doi.org/10.1016/j.aej.2018.11.005>
- Accuracy Metrics*. (2019). [http://gsp.humboldt.edu/olm\\_2019/courses/GSP\\_216\\_Online/lesson6-2/metrics.html](http://gsp.humboldt.edu/olm_2019/courses/GSP_216_Online/lesson6-2/metrics.html)
- Aljohani, T. M., Ebrahim, A. F., & Mohammed, O. (2020). Hybrid Microgrid Energy Management and Control Based on Metaheuristic-Driven Vector-Decoupled Algorithm Considering Intermittent Renewable Sources and Electric Vehicles Charging Lot. *Energies*, 13(13), Article 13. <https://doi.org/10.3390/en13133423>
- Alsomali, A., Alotaibi, F., & Al-Awami, A. (2017). *Charging strategy for electric vehicles using solar energy*. 1–5. <https://doi.org/10.1109/SASG.2017.8356485>
- Catalyst Professional – CATALYST.Earth*. (2021). <https://catalyst.earth/products/catalyst-pro/>
- Chandra Mouli, G. R., Van Duijsen, P., Grazian, F., Jamodkar, A., Bauer, P., & Isabella, O. (2020). Sustainable E-Bike Charging Station That Enables AC, DC and Wireless Charging from Solar Energy. *Energies*, 13(14), Article 14. <https://doi.org/10.3390/en13143549>
- CMP10 secondary standard pyranometer, CMP10—Kipp & Zonen*. (2010). [https://www.kippzonen.com/Product/276/CMP10-Pyranometer#.Yq\\_O1uxByUk](https://www.kippzonen.com/Product/276/CMP10-Pyranometer#.Yq_O1uxByUk)
- Duffie, J. A., & Beckman, W. A. (2013). *Solar Engineering of Thermal Processes*. John Wiley & Sons, Incorporated. <http://ebookcentral.proquest.com/lib/aucegypt/detail.action?docID=1162079>

- Duffie, J. A., Beckman, W. A., & Blair, N. (2020). *Solar Engineering of Thermal Processes, Photovoltaics and Wind*. John Wiley & Sons.
- Earth Matters—How to Pan-sharpen Landsat Imagery. (2017, June 13). [Text.Article]. NASA Earth Observatory. <https://earthobservatory.nasa.gov/blogs/earthmatters/2017/06/13/how-to-pan-sharpen-landsat-imagery/>
- Egypt: Peak load of electricity sector 2018/2019. (2021). Statista. <https://www.statista.com/statistics/1091865/egypt-amount-of-peak-load-electricity-sector/>
- EGYPT'S EVOLVING POLICY FRAMEWORK FOR ELECTRIC VEHICLES. (2020). LYNX Business Bulletin. <https://www.lynxegypt.com/assets/pdfs/EVs-Policy-Regulatory.pdf>
- Electric Vehicle Charging. (2021). <https://www.shell.com/energy-and-innovation/mobility/electric-vehicle-charging.html>
- El-Kholy, H., & Faried, R. (2011). Managing the Growing Energy Demand: The Case of Egypt. *Energy & Environment*, 22(5), 553–563. <https://doi.org/10.1260/0958-305X.22.5.553>
- Energy consumption in Egypt. (2020). WorldData.Info. <https://www.worlddata.info/africa/egypt/energy-consumption.php>
- Energy efficiency and renewable energy strategies and policies. (2019). MeetMed, European Union, RCREEE. [https://www.arabdevelopmentportal.com/sites/default/files/publication/meetmed\\_report\\_a1\\_1\\_final\\_191009.pdf](https://www.arabdevelopmentportal.com/sites/default/files/publication/meetmed_report_a1_1_final_191009.pdf)
- Estimation of the diffuse radiation fraction for hourly, daily and monthly-average global radiation—ScienceDirect. (1982). <https://www.sciencedirect.com/science/article/pii/0038092X82903024>
- Fakhraian, E., Alier, M., Valls Dalmau, F., Nameni, A., & Casañ Guerrero, M. J. (2021). The Urban Rooftop Photovoltaic Potential Determination. *Sustainability*, 13(13), Article 13. <https://doi.org/10.3390/su13137447>
- FEV Group GmbH. (2022). Development of the first Egyptian e-car by NASCO with FEV. <https://www.fev.com/en/media-center/press/press-releases/news-article/article/development-of-the-first-egyptian-e-car-by-nasco-with-fev.html>
- Gassar, A. A. A., & Cha, S. H. (2021). Review of geographic information systems-based rooftop solar photovoltaic potential estimation approaches at urban scales. *Applied Energy*, 291, 116817. <https://doi.org/10.1016/j.apenergy.2021.116817>
- Geometric Correction, Pan-sharpening and DTM Extraction – Pleiades Satellite – CATALYST.Earth. (2022). <https://catalyst.earth/2021/07/06/geometric-correction-pan-sharpening-and-dtm-extraction-pleiades-satellite/>
- Ghotge, R., Snow, Y., Farahani, S., Lukszo, Z., & van Wijk, A. (2020). Optimized Scheduling of EV Charging in Solar Parking Lots for Local Peak Reduction under EV Demand Uncertainty. *Energies*, 13(5), Article 5. <https://doi.org/10.3390/en13051275>
- GIS Mapping Software, Location Intelligence & Spatial Analytics | Esri. (2019). <https://www.esri.com/en-us/home>
- Global Solar Atlas. (2019). <https://globalsolaratlas.info/map>
- Hassan, N. M., & Abdellatif, S. O. (2021). Assessing Centralized and Decentralized EV Charging Schemes using PV-Grid Connected System, Case Study in Egypt. *2021 International Conference on Microelectronics (ICM)*, 232–235. <https://doi.org/10.1109/ICM52667.2021.9664915>
- Herold, M., Roberts, D. A., Gardner, M. E., & Dennison, P. E. (2004). Spectrometry for urban area remote sensing—Development and analysis of a spectral library from 350 to 2400 nm. *Remote Sensing of Environment*, 91(3–4), 304–319. <https://doi.org/10.1016/j.rse.2004.02.013>
- How does the tilt angle and/or orientation of the PV panel affect system performance? | Photovoltaic Lighting | Lighting Answers | NLPiP. (2021). <https://www.lrc.rpi.edu/programs/nlpip/lightinganswers/photovoltaic/14-photovoltaic-tilt-angle.asp>
- Improving Electric Vehicle Performance Using Photovoltaic Cells. (2018). <https://www.scirp.org/journal/paperinformation.aspx?paperid=86320>
- Javed, A., Cheng, Q., Peng, H., Altan, O., Li, Y., Ara, I., Huq, E., Ali, Y., & Saleem, N. (2021). Review of Spectral Indices for Urban Remote Sensing. *Photogrammetric Engineering & Remote Sensing*, 87(7), 513–524. <https://doi.org/10.14358/PERS.87.7.513>
- Kawamura, N., & Muta, M. (2012). Development of solar charging system for plug-in hybrid electric vehicles and electric vehicles. 1–5. <https://doi.org/10.1109/ICRERA.2012.6477383>
- Kosmopoulos, P., & El-Askary, H. (2019). The solar atlas of Egypt. <http://www.nrea.gov.eg/Content/files/SOLAR%20ATLAS%202018%20digital1.pdf>
- Latitude.to. (2022). GPS coordinates of American University in Cairo, Egypt. Latitude: 30.0186 Longitude: 31.5002. Latitude.to, Maps, Geolocated Articles, Latitude Longitude Coordinate Conversion. <http://latitude.to:8080/articles-by-country/eg/egypt/10935/american-university-in-cairo>

- Mohamed, S. (2018). *Comparison of Satellite Images Classification Techniques Using Landsat-8 Data for Land Cover Extraction in Alexandria, Egypt*. International Journal of Intelligent Computing and Information Science. [https://ijicis.journals.ekb.eg/article\\_194867\\_ba4b1d8f386b6b16bf0f4ee97b9b3cda.pdf](https://ijicis.journals.ekb.eg/article_194867_ba4b1d8f386b6b16bf0f4ee97b9b3cda.pdf)
- Mohammad, A., Zamora, R., & Lie, T. T. (2020). Integration of Electric Vehicles in the Distribution Network: A Review of PV Based Electric Vehicle Modelling. *Energies*, 13(17), Article 17. <https://doi.org/10.3390/en13174541>
- Muhammed, E., Morsy, S., & El-Shazly, A. (2021). Building Rooftops Extraction for Solar PV Potential Estimation Using Gis-Based Methods. *ISPRS - International Archives of the Photogrammetry, Remote Sensing and Spatial Information Sciences*, 44M3, 119–125. <https://doi.org/10.5194/isprs-archives-XLIV-M-3-2021-119-2021>
- National Solar Radiation Data Base Daily Statistics Files*. National Renewable Energy Laboratory. (2005). NREL. [http://rredc.nrel.gov/solar/old\\_data/nsrdb/dsf/](http://rredc.nrel.gov/solar/old_data/nsrdb/dsf/)
- New Administrative Capital's Map In Detail And Its Scheme*. (2019, September 24). Real Estate Egypt. <https://realestate.eg/en/blog/new-capital-compounds/new-administrative-capital-map>
- New Cairo*. (2022). [http://www.newcities.gov.eg/english/New\\_Communities/Cairo/default.aspx](http://www.newcities.gov.eg/english/New_Communities/Cairo/default.aspx)
- Pleiades-1B Satellite Sensor | Satellite Imaging Corp.* (2022). <https://www.satimagingcorp.com/satellite-sensors/pleiades-1b/>
- POLICY BRIEF: Mainstreaming Electric Mobility in Egypt: Seeing the bigger picture of sustainable cities*. (2020). Friedrich-Ebert-Stiftung. [https://egypt.fes.de/fileadmin/user\\_upload/images/FINAL\\_ENG\\_policy\\_brief\\_FES\\_online.pdf](https://egypt.fes.de/fileadmin/user_upload/images/FINAL_ENG_policy_brief_FES_online.pdf)
- Renewable Energy Outlook: Egypt*. (2018). /Publications/2018/Oct/Renewable-Energy-Outlook-Egypt. <https://www.irena.org/publications/2018/Oct/Renewable-Energy-Outlook-Egypt>
- Shaker, I., Abd-Elrahman, A., & Abdel Gawad, A. (2011). (12) (PDF) *Building Extraction from High Resolution Space Images in High-Density Residential Areas in the Great Cairo Region*. [https://www.researchgate.net/publication/228735014\\_Building\\_Extraction\\_from\\_High\\_Resolution\\_Space\\_Images\\_in\\_High\\_Density\\_Residential\\_Areas\\_in\\_the\\_Great\\_Cairo\\_Region](https://www.researchgate.net/publication/228735014_Building_Extraction_from_High_Resolution_Space_Images_in_High_Density_Residential_Areas_in_the_Great_Cairo_Region)
- Solar resource maps of Egypt*. (2019). <https://solargis.com/maps-and-gis-data/download/egypt>
- State Information Service. (2022). *The state cooperates with Egyptian scientists abroad to produce electric cars*. <https://www.sis.gov.eg/Story/167112/State-cooperates-with-Egyptian-scientists-abroad-to-produce-electric-carMohamed-Ahmed-Morsi?lang=en-us>
- Taha, L., & Elsayed, R. (2021). Assessment of Approaches for the Extraction of Building Footprints from Pléiades Images. *Geomatics and Environmental Engineering*, 15, 2021. <https://doi.org/10.7494/geom.2021.15.4.101>
- techwaves. (2019, February 13). *Centralized Solar Pool Heating System* [Text]. Solar Shams. <https://solarshams.com/content/centralized-solar-pool-heating-system>
- Tian, J., Krauß, T., & d'Angelo, P. (2017). AUTOMATIC ROOFTOP EXTRACTION IN STEREO IMAGERY USING DISTANCE AND BUILDING SHAPE REGULARIZED LEVEL SET EVOLUTION. *The International Archives of the Photogrammetry, Remote Sensing and Spatial Information Sciences*, XLII-1/W1, 393–397. <https://doi.org/10.5194/isprs-archives-XLII-1-W1-393-2017>
- Twidell, J., & Weir, T. (1986). *Renewable energy resources* (second).
- Vermeer, W., Chandra Mouli, G. R., & Bauer, P. (2020). Real-Time Building Smart Charging System Based on PV Forecast and Li-Ion Battery Degradation. *Energies*, 13(13), Article 13. <https://doi.org/10.3390/en13133415>
- Xiang, Y., Sun, Y., & Li, C. (2012). A Rooftop Extraction Method Using Color Features, Height Map Information, and Road Information. *Proceedings of SPIE - The International Society for Optical Engineering*, 8537. <https://doi.org/10.1117/12.974443>
- ZuWhan Kim, Huertas, A., & Nevatia, R. (2001). Automatic description of buildings with complex rooftops from multiple images. *Proceedings of the 2001 IEEE Computer Society Conference on Computer Vision and Pattern Recognition. CVPR 2001*, 2, II-272-II-279. <https://doi.org/10.1109/CVPR.2001.990971>